CrystEngComm

Accepted Manuscript

This is an *Accepted Manuscript*, which has been through the Royal Society of Chemistry peer review process and has been accepted for publication.

Accepted Manuscripts are published online shortly after acceptance, before technical editing, formatting and proof reading. Using this free service, authors can make their results available to the community, in citable form, before we publish the edited article. We will replace this *Accepted Manuscript* with the edited and formatted *Advance Article* as soon as it is available.

You can find more information about *Accepted Manuscripts* in the Information for Authors.

Please note that technical editing may introduce minor changes to the text and/or graphics, which may alter content. The journal's standard Terms & Conditions and the Ethical guidelines still apply. In no event shall the Royal Society of Chemistry be held responsible for any errors or omissions in this *Accepted Manuscript* or any consequences arising from the use of any information it contains.

ROYAL SOCIETY OF CHEMISTRY

www.rsc.org/crystengcomm

CrystEngComm

PAPER

Coordination networks incorporating halogen-bond donor sites and azobenzene groups

Received 00th January 20xx,
Accepted 00th January 20xx

DOI: 10.1039/x0xx00000x

www.rsc.org/

Francisco Fernandez-Palacio,[a] Marco Saccone,[b] Arri Priimagi,[b] Giancarlo Terraneo,[a] Tullio Pilati,[a] Pierangelo Metrangolo[a,c]* and Giuseppe Resnati[a]*

Two Zn coordination networks, {[Zn(**1**)(Py)$_2$]$_2$(2-propanol)}$_n$ (**3**) and {[Zn(**1**)$_2$(Bipy)$_2$](DMF)$_2$}$_n$ (**4**), incorporating halogen-bond (XB) donor sites and azobenzene groups have been synthesized and fully characterized. The obtainment of **3** and **4** confirms that it is possible to use a ligand where coordination bond acceptor sites and XB donor sites are on the same molecular scaffold (*i.e.*, an aromatic ring) without interfering with each other. We demonstrate that XB plays a fundamental role in the architectures and properties of the obtained coordination networks. In **3**, XBs promote the formation of 2D supramolecular layers, which, by overlapping each other, allow for the incorporation of 2-propanol as a guest molecule. In **4**, XBs support the connection of the layers and are essential to firmly pin DMF solvent molecules through I···O contacts, thus increasing the stability of the solvated systems.

Introduction

In depth understanding of intermolecular interactions that govern crystal packing in solids is a hot topic in present-day research due to its instrumental role in the design and synthesis of new materials.[1] In particular, the use of metals in crystal engineering has attracted considerable attention and led in recent years to the development of entirely new classes of materials such as coordination polymers[2] (CPs) and Metal Organic Frameworks (MOFs).[2,3] The interest in these systems is related to their easy structural and functional tunability that allows for a plethora of applications in quite different fields, such as gas adsorption and separation,[4] catalysis,[5] molecular recognition,[6] medical diagnosis, and therapy.[7]

Decorating the structure of ligands compounding CPs and MOFs with tailored functionalities is a pivotal strategy to control and tune their functional properties.[8] For instance, ligands possessing azobenzene moieties[9] have been used to assemble MOFs capable of releasing small molecules under solid,[10] liquid,[11] or gaseous[12] conditions thanks to the clean and reversible photoisomerization of the azobenzene group, enabling the precise control of the opening of the MOFs' pores. Complementarily, selective capture and release of hosted molecules can be obtained by decorating cavities and pores of frameworks with a given functionality, capable of specifically interacting with a complementary functionality of guest molecules that are then retained by the MOFs with greater affinity than unfunctionalized analogues.

With this objective in mind, our molecular design was based on the well-known ligand 5-amino-2,4,6-triiodoisophthalic acid (H2atiip, Fig.1, left), which has already shown its potential in the formation of MOFs and CPs.[13,14] Furthermore, H2atiip has three I atoms that are potential donor sites for halogen bonding (XB),[15] which is the attractive interaction between an electrophilic region of a halogen atom in a molecular entity and a nucleophilic region in another, or the same, molecular entity.[16] Finally, the NH_2 group of H2atiip allows for the introduction of the photoresponsive azo moiety into the organic ligand. We reasoned that the combination of a photoresponsive moiety in the ligand and pore decoration with XB-donor groups, could offer extra opportunities for the controlled capture and release of guest molecules.

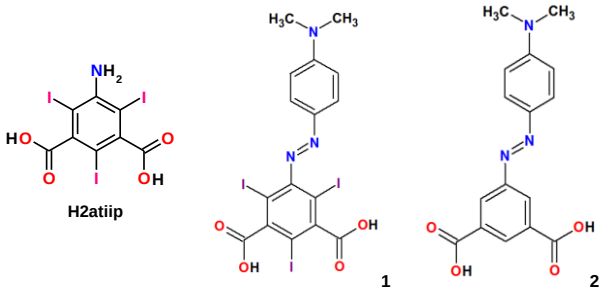

Fig. 1. The azobenzene dicarboxylates **1** and **2** used as ligands in this work.

Motivated by our recent results[17] in using azobenzene molecules containing XB-donor sites, we report here on the new organic ligand **1** (Fig.1, centre) containing azo- and iodo-benzene moieties, and the zinc(II) coordination polymers obtained thereof. By preparing CPs containing both azo- and iodo-benzene moieties, we aimed at assessing whether the

[a] *NFMLab-DCMIC "Giulio Natta", Politecnico di Milano, Via L. Mancinelli 7, 20131 Milano, Italy.*
E-mail: pierangelo.metrangolo@polimi.it; giuseppe.resnati@polimi.it
[b] *Department of Chemistry and Bioengineering, Tampere University of Technology, P.O. Box 541, FI-33101 Tampere, Finland.*
[c] *VTT-Technical Research Centre of Finland, Espoo FI-02044, Finland.*
† Electronic Supplementary Information (ESI) available: Single crystal diffraction refinement details and photochemical studies. See DOI: 10.1039/c000000x/

binding/release of a hosted molecule can be tuned *via* XB formation or by a rearrangement of the azo moiety or by a combination of these two factors. In order to demonstrate this, we also prepared an analogous network by using ligand **2**, the non-iodinated parent of **1**.

Experimental Section

Materials and Methods

All reagents and solvents were purchased from Aldrich and used without further purification. ^{1}H and ^{13}C NMR spectra were recorded at room temperature on a Bruker AV400 spectrometer. ^{1}H NMR and ^{13}C NMR chemical shifts were referenced to tetramethylsilane (TMS) using the residual proton impurities of the deuterated solvents as standard reference. Melting points were determined on a Reichert instrument by observing the melting process though an optical microscope. ATR-FTIR spectra were obtained with a Nicolet Nexus FTIR spectrometer. The values, given in wave numbers, were rounded to 1 cm^{-1} using automatic peak assignment. Mass spectra were recorded on a BRUKER Esquire 3000 PLUS.

Synthetic Procedures

(*E*)-4-((2,4,6-triiodoisophtalic)phenyl)diazenyl)-*N*,*N*-dimethylbenzenamine (1). In a round bottom flask 5-amino-2,4,6triiodosophtalic acid (0.560 g, 1 mmol) was dissolved in 3 ml of water. The solution was cooled to -3^{o} C. After 10 minutes, 0.3 mL of concentrated HCl were added. In an Erlenmeyer flask, sodium nitrite (1 eq) was dissolved in 0.8 mL of water and cooled at the same temperature. The two solution were combined at -3^{o} C under vigorous stirring. Sodium acetate and *N,N*–dimethylaniline were than dissolved in a mixture of ethanol and water (2 mL : 0.8 mL). This solution was also cooled down to -3^{o}C and added, over 20 minutes, to the amine solution. The reaction was stirred for 16 hours at room temperature. Water was added and the mixture was extracted tree times with ethyl acetate. The solution was dried (Na_2SO_4) and evaporated under vacuum. After that, a solution of NaOH (0.01 M) was added to the solid. The resulting solution was washed several times with ethyl acetate. Then aqueous solution was acidified with HCl (pH=1). Finally, the mixture was extracted with ethyl acetate (for two times) and the solvent was removed under vacuum. **1** was obtained as a red solid in 55% yield.
Melting point: 237^{o} C (dec.). ^{1}H NMR (DMSO-d_6, 400 MHz, 293 K, δ ppm): 7.81 (d, $^{3}J_{HH}$ = 8 Hz, 2H), 6.88 (d, $^{3}J_{HH}$ = 8 Hz, 2H), 3.10 (s, 6H). ^{13}C NMR (DMSO-d_6, 100 MHz, 293 K, δ ppm): 169.21, 148.96, 147.19, 146.55, 141.26, 140.18, 125.31, 111.45, 92.59, 88.90, 85.67, 30.54. ATR-FTIR: ν_{max} = 3323, 2911, 2637, 2504, 1729, 1697, 1598, 1545, 1516, 1317, 1248, 1179, 1126, 931,917, 902, 750 cm^{-1}. Anal. Calcd for $C_{16}H_{12}N_3O_4I_3$: C, 27.81; H, 1.75; N, 6.08%. Found: C, 27.62; H, 1.72; N, 5.99%. MS/ESI *m/z* 691.0, found 692.1 (M + H^{+}).

(*E*)-4-(isophtalicphenyl)diazenyl)-*N*,*N*-dimethylbenzenamine (2). This compound was synthetized using the same procedure applied for **1**. The 5-amino-2,4,6-triiodosophtalic acid was substituted with 5-aminoisophtalic acid (1 mmol). **2** was obtained as a red solid in 62% yield.
Melting point: 251^{o} C (dec.). ^{1}H NMR (DMSO-d_6, 400 MHz, 293 K, δ ppm): 8.47 (s, 1H). 8.45 (s, 2H), 7.85 (d, $^{3}J_{HH}$ = 8 Hz, 2H), 6.85 (d, $^{3}J_{HH}$ = 8 Hz, 2H), 3.08 (s, 6H). ^{13}C NMR (DMSO-d_6, 100 MHz, 293 K, δ ppm): 166.70, 153.60, 153.25, 142.94, 132.97, 130.44, 126.43, 125.80, 112.10. ATR-FTIR: ν_{max} = 2819, 2663, 2549, 1692, 1602, 1562, 1522, 1454, 1397, 1366, 1277, 1148, 916, 813, 858, 726, 692 cm^{-1}. Anal. Calcd for $C_{16}H_{15}N_3O_4$: C, 61.34; H, 4.83; N, 13.41%. Found: C, 61.11; H, 4.63; N, 13.67%. MS/ESI *m/z* 313.3, found 314.1 (M + H^{+}).

$\{[Zn(1)(Py)_2]_2(2\text{-propanol})\}_n$ (3). A mixture of 0.032 g (0.107 mmol) of $Zn(NO_3)_2{\cdot}6H_2O$, 0.036 g (0.052 mmol) of **1**, 0.009 g (0.106 mmol) of pyridine (Py), 0.053 mL of a solution 2M (NaOH in H_2O) and 0.132 mL of 2-propanol was sealed in a 1.5 mL Teflon-lined autoclave and heated at 80 °C for 32 hours. Then the autoclave was slowly cooled down to room temperature. The mixture was filtered and compound **3** was isolated as red crystals.

Synthesis of $\{[Zn(1)_2(Bipy)_2](DMF)_2\}_n$ (4). A mixture of 0.008 g (0.027mmol) of $Zn(NO_3)_2.6H_2O$, 0.012g (0.0179 mmol) of **1**, 0.010g (0.064 mmol) of 4,4'-bipyridine (Bipy) was dissolved in 5 mL of DMF, 2 mL of ethanol and 1 mL of H_2O. The solution was stirred for 10 min. The mixture was filtered and kept at room temperature. After some days, a red single crystal was obtained.

Synthesis of $\{[Zn(2)(Bipyeth)](DMF)_{1.81}\}_n$ (5). 0.008 g (0.027 mmol) of $Zn(NO_3)_2.6H_2O$, 0.006g (0.0179 mmol) of **2**, 0.012g (0.064 mmol) of di(4-pyridyl)ethylene (Bipyeth) were dissolved in 5 mL of DMF, 2 mL of ethanol and 1 mL of H_2O. The mixture was stirred for 10 min. After that, it was filtered and kept at room temperature. After some days compound **5** was isolated as red crystals.

Crystal Structure Determination

The single crystal X-Ray structures of **3-5** were determined on a Bruker Kappa Apex II diffractometer at 103 K using a fine-focus MoKα tube, λ=0.71073 Å. Data collection and reduction were performed by SMART and SAINT and absorption correction, based on multi-scan procedure, by SADABS. The structure were solved by SHELXL2008[18] and refined on all independent reflections by full-matrix least-squares based on F^2 by using SHELX-2008.[18] All the non-hydrogen atoms were refined anisotropically. Hydrogen atoms were placed in calculated positions and refined by using a riding model. Crystallographic data and structural refinement details are summarized in Table 1. Further experimental details on how twinning and molecular disorder were treated are given in ESI†. Crystallographic data for the structural analysis have been deposited with the Cambridge Crystallographic Data Center. Figures are obtained with Mercury 3.5.[19]

Structure	3	4	5
Chemical formula	$2C_{26}H_{20}I_3N_5O_4Zn\bullet C_3H_8O$	$C_{52}H_{38}I_6N_{10}O_8Zn\bullet 2C_3H_7NO$	$C_{28}H_{23}N_5O_4Zn\bullet 1.81C_3H_7NO$
Formula weight	1885.17	1903.89	690.97
Temperature K	103(2)	103(2)	103(2)
Crystal system	Monoclinic	Monoclinic	Monoclinic
Space group	$P2_1/n$	$C2/c$	$P2_1/c$
a (Å)	8.813(2)	24.0554(18)	10.1389(5)
b (Å)	23.763(5)	11.3346(9)	14.9139(8)
c (Å)	14.620(3)	22.9563(18)	23.1236(12)
α (°)	90.00	90.00	90.00
β (°)	91.91(2)	98.893(8)	95.194(2)
γ (°)	90.00	90.00	90.00
Volume (Å^3)	3060.1(11)	6184.0(8)	3482.2(3)
Z	2	4	4
Density (g cm^{-3})	2.046	2.045	1.316
μ (cm^{-1})	3.873	3.461	0.757
Dimensions (mm^{-3})	0.04, 0.04, 0.21	0.06, 0.07, 0.33	0.07, 0.14, 0.21
Colour, form	Red, needle	Red, needle	Orange, prism
Absorption correction	0.5437, 0.6752	0.4380, 0.5769	0.6977, 0.7456
T_{min},T_{max}			
Collected reflections	35345	58923	77266
Unique reflections	5805	10264	7964
Reflections with $I_o > \sigma(I_o)$	4236	8277	5474
R_{ave}	0.068	0.050	0.041
θ_{max}	25.68	31.51	27.91
Parameters, restraints	409, 142	483, 229	431, 406
R_1 [all, $I_o > 2\sigma(I_o)$]	0.077,0.049	0.063, 0.048	0.115, 0.079
wR_2 [all, $I_o > 2\sigma(I_o)$]	0.115, 0.104	0.130, 0.122	0.257, 0.227
Goodness of fit	1.040	1.037	1.057
$\Delta\rho$ (min,max)	-2.00, 4.29	-3.65, 2.72	-0.64, 0.95
CCDC number	1445292	1445293	1445294

Table 1 Crystallographic data and structure refinement parameters for **3**-**5**.

Photochemistry

The UV-Vis spectra were collected from both films and diluted (10^{-5} M) DMF solutions with an Oceans Opticals USB2000+ fiber-optic spectrometer and a DH-2000-BAL light source, both in dark and under irradiation (457 nm, 50 mW/cm^2). Thermal *trans-cis* isomerization was studied by exciting the chromophores to the *cis*-state with a circularly polarized pump beam (457 nm, 50 mW/cm^2) and monitoring the transmittance changes after blocking the pump. The probe was a fiber-coupled xenon lamp equipped with proper bandpass filters. The signal was detected with a photodiode and a lock-in amplifier. See ESI for discussion and graphics.

Results and Discussion

The azobenzene ligands **1** and **2** were synthesized by diazotization of H2atiip followed by reaction with *N*,*N*-dimethylaniline.[20] Both **1** and **2** possess a dimethylamino group on one benzene ring and two carboxylic groups on the other; three iodine atoms being present in **1** only. Zn(II) was chosen to prepare the CPs described here because it is air stable and easy to handle,[21] and its complexes are among the most stable in the Irving-Williams series.[22]

The hydrothermal reaction[23] involving **1**, $Zn(NO_3)_2{\cdot}6H_2O$, 2-propanol, and pyridine (Py), afforded the CP $\{[Zn(\mathbf{1})(Py)_2]_2(2\text{-propanol})\}_n$ (**3**) that was isolated as red crystals suitable for single-crystal X-ray diffraction (XRD) analysis. CP **3** comprises $[Zn(\mathbf{1})](Py)_2]_n$ 1D chains developing along the [1,0,-1] direction (Fig. 2A). The Zn nodes adopt a tetrahedral geometry and adjacent cations are bridged by the same dicarboxylate ligand **1**. The resulting 1D chains are functionalized by two pyridines, which saturate the tetrahedral coordination geometry of zinc cations.

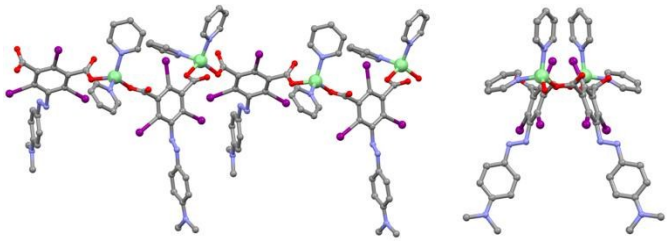

Fig. 2. Two different representations of the 1D coordination chain formed by Zn, ligand **1**, and pyridine units in **3**. View approximately orthogonal (left) and along (right) the chain main axis. Hydrogen atoms are omitted for clarity. Color code: grey, carbon; sky blue, nitrogen; red, oxygen; violet, iodine; light green, zinc.

All the azo-ligands in **3** are oriented on the same side of the plane defined by the Zn atoms, while half of the pyridine molecule lie in this plane and the other half is located on the opposite side of **1** (Fig. 2).

In the obtained 1D chains, each azobenzene molecule **1** bridges two metal cations through its two carboxylate groups, which function as monodentate binding sites, Zn(1)-O(1) and Zn(1)-O(3)^i (i = -1/2+x,1/2-y,-1/2+z) distances are 1.939(5) and 1.946(5) Å, respectively. The adjacent chains are linked together forming a 2D layered structure through I(1)···I(2)^i XB (i = -1/2+x,1/2-y,-1/2+z, I···I distance is 3.7259(10) Å, C-I···I and I···I-C angles are 160.7(2)° and 115.1(2)°, respectively, Fig. 3A). The halogen-bonded layers are superposed and interact with each other only through very weak hydrogen bonds (HBs) occurring between I(3)···H(15)b (3.06 Å, Fig. 3B). The resulting supramolecular network presents voids (234 Å^3 per unit cell) that are filled by two disordered 2-propanol molecules (see ESI).

We reasoned that a bidentate pyridine unit, such as 4,4'-bipyridyl (Bipy), could allow for the obtainment of networks with higher dimensionality than **3**. We therefore reacted **1** and $Zn(NO_3)_2{\cdot}6H_2O$ with Bipy. After several days at room temperature, a solution of **1** and $Zn(NO_3)_2{\cdot}6H_2O$ in a mixture of dimethylformamide (DMF), EtOH, and water, afforded deep red crystals of the framework $\{[Zn(\mathbf{1})_2(Bipy)_2](DMF)_2\}_n$ (**4**), whose structure was revealed by single-crystal XRD.

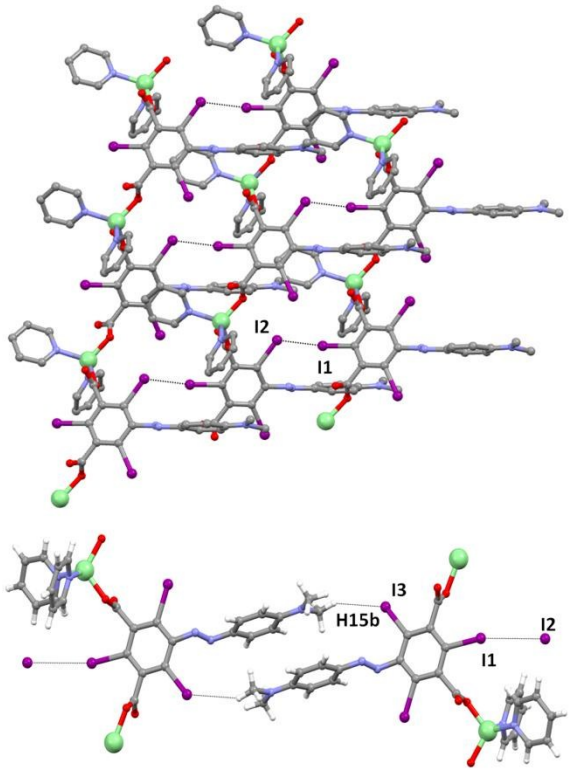

Fig. 3. Top: Representation of the 2D layer structure of **3** formed by halogen bonds. Bottom: Representation of the hydrogen bonding motif responsible for the interaction between halogen-bonded layers. XBs and HBs are in black dotted lines. Color code as in Fig. 2, hydrogen atoms are in white.

Despite the poor quality of the data, the structural features of the self-assembled system were unequivocally determined. Specifically, both the bipyridyl and benzenedicarboxylate units were split over different positions with quite unbalanced refined population factors, probably as a consequence of severe crystal twinning (see ESI).

In **4**, Zn cations adopt an octahedral coordination with two azobenzene dicarboxylate units **1** in axial positions and four bipyridyl molecules in equatorial positions (N···Zn···N angles are 82.30 and 97.70°). This arrangement produces a non-interpenetrating (4,4) network where Zn atoms are the nodes and bipyridyl units function as spacers (Fig. 4). The resulting network shows a planar and distorted-square geometry with a crystallographic twofold symmetry; the sides of the parallelograms in the network being 11.842 and 11.335 Å long. The octahedral coordination at each node of the (4,4) network is completed by two molecules of the ligand **1** that enter from opposite sides and nearly orthogonal to the 2D network (O···Zn···N angles in the range 92.38°-87.20°). Notably only one of the two carboxylates is bound to zinc, while the other one interacts through weak HBs with adjacent nets.

The *N*,*N*-dimethylaminophenyl pendants of ligands **1** align almost parallel to the shortest diagonal of the parallelograms of the (4,4) network and are oriented above and below these parallelograms. This arrangement creates isolated boxes, which are nicely decorated with iodine atoms ready to work as XB-donor sites. Indeed, two symmetry-related DMF molecules are hosted in these cavities and are pinned to their positions through quite short and directional C-I···O XBs [I(1)···O distance is 2.942(5) Å, C-I···O angle is 175.41(11)°] (Fig. 5). This distance corresponds to a normalized contact (N_c)[24] of 0.84, which is among the shortest observed in cocrystals between iodobenzene derivatives and carbonyl groups.[25]

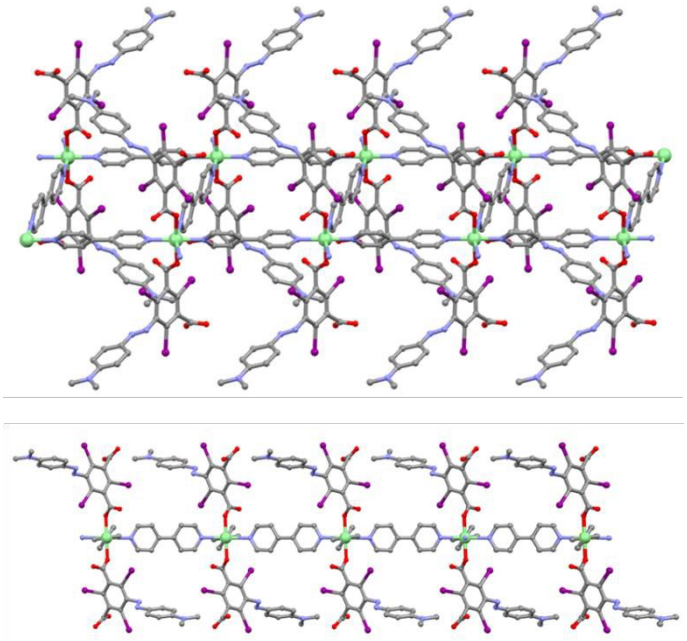

Fig. 4. Representation of one (4,4) network in **4**, seen quasi-orthogonal to (top) and along (bottom) the *b* crystallographic axis. The top representation highlights how the dimethylaminophenyl groups lie above and below the parallelograms of the net and delimit the box wherein the DMF molecules are captured. In the bottom representation, the ligand **1** units have been deleted to highlight the planar and distorted-square geometry of the coordination network. Disorder on the ligand **1**, hydrogen atoms, and DMF molecules have been omitted for clarity. Color code as in Fig. 2.

This fairly short separation is the probable consequence of a subtle balance of various structural and electronic factors. First, the volume of the cavity hosting the two DMF molecules is 166 Å^3 (as calculated with Mercury 3.5, probe radius 1.2 Å), while the volume that these two molecules are expected to occupy is 204 Å^3 (estimated from the volume of the unit cell of pure DMF, CSD Refcode KAQPUN[26]). DMF being tightly packed in the cavities, congestion may prevent its motion and force it closer to the cavity walls, so that short XBs may result. Moreover, while the iodine and oxygen atoms involved in the interaction are expected to be medium strength XB-donors and -acceptors in their respective categories,[27] the C-I···O XBs occur in the confined space of a framework cavity. It is known that the molecular motion of guest molecules confined in a cavity are reduced so that the manifestation of weak intermolecular contacts, in this case the XB, is favored and its properties enhanced.[28] Thanks to the combination of all these conditions, the DMF molecules in **4** are effectively blocked in their positions and are not disordered.

Another distinctive feature of **4** is the occurrence of an XB between one of the nitrogen atoms of the azo moiety and one of iodine atoms present on a nearby ligand **1** (Fig. 5); I(3)···N(2) distance and C-I···N angle are 2.974(3) Å (N_c = 0.84) and 166.79(10)°, respectively. This contact is quite short and especially if compared to the only other XB found in the CSD and involving an iodine atom and an azo group (Refcode: TEGFUI; 3.240 Å (Nc = 0.95), 152.5°).[29] This short contact is rather unexpected as nitrogen atoms of the azo moiety are only mildly basic and thus poor XB-acceptors.[30] Probably, the tight proximity imposed by the network conveniently pre-organizes the interacting units and favors the occurrence of a relatively short XB.

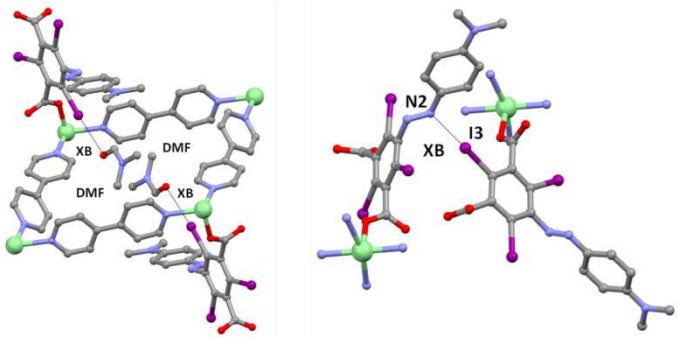

Fig. 5. Left: Partial view of the isolated box in **4** where two symmetry-related DMF molecules are pinned through I···O XBs. Part of the (4,4) network and hydrogen atoms are omitted for clarity. Right: XB occurring between one nitrogen atom on the azo group and an iodine atom on ligand **1**. XBs are in black dotted lines. Color code as in Fig. 2.

In order to assess the role of the XB in effectively pinning DMF molecules in place in the above-described networks, ligand **2** (Fig.1, right), the non-iodinated parent of **1**, was reacted with $Zn(NO_3)_2{\cdot}6H_2O$, and (*E*)-1,2-di(4-pyridyl)ethylene (Bipyeth) using the same solvent mixture and under the same conditions applied for **4**. The framework $\{[Zn(\mathbf{2})(Bipyeth)](DMF)_{1.81}\}_n$ (**5**) was obtained and its structure was established via single-crystal XRD analysis.

In **5** the Zn atoms adopt a tetrahedral coordination, adjacent cations are bridged by the carboxylate moieties present on ligands **2**, and 1D coordination polymer chains, strongly resembling those found in **3**, are formed.

The use of a ditopic ligand, which saturates the tetrahedral coordination geometry around Zn atoms, allows for the connection of the chains and the obtainment of an undulated 2D (4,4)-network where metal cations are the nodes and dicarboxylate ligands and Bipyeth molecules act as alternating sides (Fig. 6). Geometrical parameters of the parallelogram in the (4,4)-network are as follows: sides 10.139 and 13.382 Å long and the angles 85.51° and 94.49°.

In the coordination layer, the *N*,*N*-dimethylaminophenylazo residues of the ligand **2** stick out of the undulated sheet in an alternating up-down fashion. This peculiar arrangement allows for the interdigitation of adjacent layers, which creates an extended framework with voids (Fig. 7).

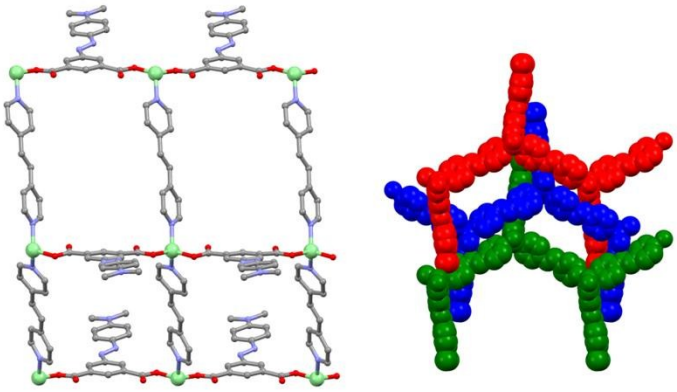

Fig. 6. Left: Representation of one (4,4) network in **5** along the *b* crystallographic axis. Disorder on the ligand **2**, hydrogen atoms, and DMF molecules have been omitted for clarity. This view highlights how the dimethylaminophenylazo groups lie above and below the parallelogram layers. Color code as in Fig. 2. Right: The interdigitation of three 2D layers projected along *a* axis is highlighted using different colors.

Differently from **4** where the cavities are isolated, the overall 3D architecture in **5** promotes the formation of a rectangular grid of pipes occupied by DMF solvent molecules (Fig. 7). However, the number of guest molecules accommodated in **5** is smaller than in **4** (only 1.81 per [Zn(**2**)(Bipyeth)] unit) and only one molecule of DMF is

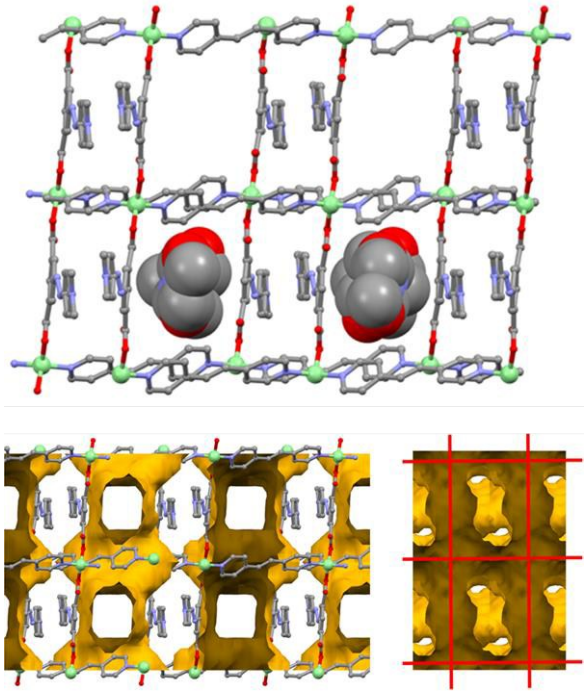

Fig. 7. Top Representation of (4,4) networks in **5** along the *b* crystallographic axis. DMF molecules (reported in one layer only) are in space filling representation. Bottom, left: Representation of the contact surface (dark yellow) of the rectangular grid networks of voids calculated using a spherical "probe" of 1.2 Å, viewed along the *b* crystallographic axis. The DMF molecules are omitted. Bottom, right: View of the contact surface (dark yellow) area of the rectangular grid networks in the *ac* plane. Red lines highlight the grid topology. Color code as in Fig. 2.

crystallographically ordered. This difference clearly reveals that XBs between hosted DMF molecules and hosting metal-organic framework being absent, DMF molecules are less tightly bound in **5** than in **4**. Interestingly, during the XRD experiments all the crystals of **5** underwent a fast decay, due to the loss of DMF molecules, with relative decrease of the collected data quality. This rapid loss of crystallinity of all the analyzed crystals of **5** is a further indication of the key role of XB in trapping DMF molecules in **4**.

Conclusions

In summary, we obtained three new coordination polymers based on Zn(II) nodes and azo-benzene carboxylate ligands, which display different architectures, $\{[Zn(\mathbf{1})(Py)_2]_2(2\text{-propanol})\}_n$ (**3**), $\{[Zn(\mathbf{1})_2(Bipy)_2](DMF)_2\}_n$ (**4**), and $\{[Zn(\mathbf{2})(Bipyeth)](DMF)_{1.81}\}_n$ (**5**). The obtainment of **3** and **4** confirms that it is possible to use a ligand where coordination bond acceptor sites and halogen-bond donor sites are on the same molecular scaffold (*i.e.*, an aromatic ring) without interfering with each other. This strategy is general and, in our experiments, worked both in hydrothermal and isothermal conditions.

Halogen bonding plays a fundamental role in the architectures and properties of the obtained CPs. In **3**, XBs promote the formation of 2D supramolecular layers, which, by overlapping each other, allow for the incorporation of 2-propanol as a guest molecule. In **4**, XBs support the connection of the layers and are essential to firmly pin DMF solvent molecules through I···O contacts, thus increasing the stability of the solvated systems. This important role is highlighted by the different behavior of **5** where the absence of XB-donor sites on the ligand reduces the ability of the framework to host DMF molecules and the overall stability of the entire system.

The photochemical properties of the CPs are still under investigation but photoisomerization of **1** and **2** in solution (see ESI) already shows that iodination significantly affects both the *cis*-isomer fraction of the azobenzene in the photostationary state and its lifetime (*i.e.*, τ = 3000 s and τ = 850 s for **1** and **2**, respectively). The properties in the solid state will be further affected by the intermolecular contacts present in the CPs. For controlled release of a guest, bistable switching is of benefit, which may be achieved through proper *ortho*-substitution[31] and the removal of the dimethylamino groups. Such outcomes are important in view of the design and synthesis of future halogen-bonded azobenzene-containing photoresponsive coordination networks.

Acknowledgements

PM and GT acknowledge support from the MIUR, PRIN 2010-2011 (grant 2010CX2TLM "InfoChem").

References

1 G. R. Desiraju, J. J. Vittal and A. Ramanan, *Crystal Engineering: A Textbook*, World Scientific, Singapore, 2012.
2 S. R. Batten, N. R. Champness, X.-M. Chen, J. Garcia-Martinez, S. Kitagawa, L. Öhrström, M. O'Keeffe, M. P. Suh and J. Reedijk, *Pure Appl. Chem*. 2013, **85**, 1715.
3 (a) O. M. Yaghi, M. O'Keeffe, N. W. Ockwig, H. K. Chae, M. Eddaoudi and J. Kim, *Nature*, 2003, **423**, 705; (b) H. Furukawa, K. E. Cordova, M. O'Keeffe and O. M. Yaghi, *Science*, 2013, **341**, 974.
4 J.-R. Li, R. J. Kuppler and H.-C. Zhou, *Chem. Soc. Rev.*, 2009, **38**, 1477.
5 M. Yoon, R. Srirambalaji, and K. Kim, *Chem. Rev.*, 2010, **112**, 1196.
6 B. Chen, S. Xiang and G. Qian, *Acc. Chem. Res*., 2010, **43**, 1115.
7 A. C. McKinlay, R. E. Morris, P. Horcajada, G. Férey, R. Gref, P. Couvreur and C. Serre, *Angew. Chem. Int. Ed*., 2010, **49**, 6260.
8 (a) Y. Cui, Y. Yue , G. Qian and B. Chen, *Chem. Rev*., 2012, **112**, 1126; (b) M. Kurmoo, *Chem. Soc. Rev*., 2009, **38**, 1353; (c) M. Servati-Gargari, G. Mahmoudi, S. R. Batten, V. Stilinović, D. Butler, L. Beauvais, W. S. Kassel, W. G. Dougherty, and D. VanDerveer, *Cryst. Growth Des.,* 2015, **15**, 1336.
9 (a) O. S. Bushuyev, T. C. Corkery, C. J. Barrett, and T. Friščić, *Chem. Sci.,* 2014, **5**, 3158; (b) O. S. Bushuyev, D. Tan, C. J. Barrett, and Tomislav Friščić, *CrystEngComm,* 2015, **17**, 73; (c) O. S. Bushuyev, A. Tomberg, T. Friščić, and C. J. Barrett, *J. Am. Chem. Soc.,* 2013, **135**, 12556.
10 J. W. Brown, B. L. Henderson, M. D. Kiesz, A. C. Whalley, W. Morris, S. Grunder, H. Deng, H. Furukawa, J. I. Zink, J. F. Stoddart and O. M. Yaghi, *Chem. Sci*. 2013, **4**, 2858.
11 L. Heinke, M. Cakici, M. Dommaschk, S. Grosjean, R. Herges, S. Bräse, and C. Wöll, *ACS Nano*, 2014, **8**, 1463.
12 R. Lyndon, K. Konstas, B. P. Ladewig, P. D. Southon, C. J. Kepert and M. R. Hill, *Angew. Chem. Int. Ed*., 2013, **52**, 3695.
13 F. Dai, H. He, X. Zhao, Y. Ke, G. Zhang and Daofeng Sun, *CrystEngComm*, 2010, **12**, 337.
14 K.-L. Zhang, Y. Chang, C.-T. Hou, G.-W. Diao, Rentao Wu and Seik Weng Ng, *CrystEngComm*, 2010, **12**, 1194.
15 G. R. Desiraju, P. S. Ho, L. Kloo, A. C. Legon, R. Marquardt, P. Metrangolo, P. Politzer, G. Resnati and K. Rissanen, *Pure Appl. Chem*., 2013, **85**, 1711.
16 (a) M. Saccone, G. Cavallo, P. Metrangolo, A. Pace, I. Pibiri, T. Pilati, G. Resnati and G. Terraneo, *CrystEngComm*, 2013, **15**, 3102; (b) D. Cinčić, and T. Friščić, *CrystEngComm,* 2014, **16**, 10169; (c) D. Cinčić, T. Friščić, and W. Jones, *J. Am. Chem. Soc.,* 2008, **130**, 7524.
17 (a) M. Saccone, V. Dichiarante, A. Forni, A. Goulet-Hanssens, G. Cavallo, J. Vapaavuori, T. Pilati, G. Terraneo, G. Resnati, P. Metrangolo and A. Priimagi *J. Mater. Chem. C*, 2015, **3**, 759; (b) M. Virkki, O. Tuominen, A. Forni, M. Saccone, P. Metrangolo, G. Renati, M. Kauranen and A. Priimagi, *J. Mater. Chem.* C, 2015, **3**, 3003; (c) M. Saccone, G. Terraneo, T. Pilati, G. Cavallo, A. Priimagi, P. Metrangolo and G. Resnati, *Acta Crystallogr. B*, 2014, **B70**, 149.
18 G. M. Sheldrick, *Acta Crystallogr.* 2008, **A64**, 112.
19 C. F. Macrae, P. R. Edgington, P. McCabe, E. Pidcock, G. P. Shields, R. Taylor, M. Towler, and J. van de Streek, *J. Appl. Crystallogr.* 2006, **39**, 453.
20 A. Priimagi, M. Saccone, G. Cavallo, A.Shishido, T. Pilati, P. Metrangolo and G. Resnati, *Adv. Mater.*, 2012, **24**, OP345.
21 (a) F. Fernandez-Palacio, J. Restrepo, S. Galvez, P. Gomez-Sal and M. E. G. Mosquera, *CrystEngComm*, 2014, **16**, 3376; (b) N. Getachew, Y. Chebude, I. Diaz, M. Sanchez-Sanchez, *J. Porous Mater*., 2014, **21**, 769.
22 H. Irving and R. J. P. Williams, *J. Chem. Soc.*, 1953, 3192.
23 O. M. Yaghi and H. Li, *J. Am. Chem. Soc*., 1995, **117**, 10401.

24 We define 'normalized contact', the ratio $N_c = D_{ij}/(r_{vdWi} + r_{vdWj})$, where D_{ij} is the experimental distance between the atoms i and j and r_{vdWi} and r_{vdWj} are the van der Waals radii for atoms I and J.

25 201 Structures with 252 I···O contacts shorter than the sum of iodine and oxygen van der Waals radii were found in the Cambridge Structural Database (version 5.36). Only twelve of them are shorter than the contact in **4**, nine being in homocrystals and three in cocrystals (IPOSIP, TOJCEP, and YUTWAM) where iodoperfluorobenzenes are the XB-donors.

26 H. Borrmann, I. Persson, M. Sandström, and C. M. V. Stålhandskeb, *J. Chem. Soc., Perkin Trans. 2,* 2000, 393.

27 S. K. Nayak, G. Terraneo, A. Forni, P. Metrangolo and G. Resnati *CrystEngComm*, 2012, **14**, 4259.

28 (a) M. G. Sarwar, D. Ajami, G. Theodorakopoulos, I. D. Petsalakis, and J. Rebek Jr., *J. Am. Chem. Soc.*, 2013, **135**, 13672; (b) H. Takezawa, T. Murase, G. Resnati, P. Metrangolo and M. Fujita, *Angew. Chem. Int. Ed*., 2015, **54**, 8411.

29 A. Priimagi, G. Cavallo, A. Forni, M. Gorynsztejn-Leben, M. Kaivola, P. Metrangolo, R. Milani, A. Shishido, T. Pilati, G. Resnati and G. Terraneo, *Adv. Funct. Mater.*, 2012, **22**, 2572.

30 D. Fox, P. Metrangolo, D. Pasini, T. Pilati, G. Resnati and G. Terraneo, *CrystEngComm*, 2008, **10**, 1132.

31 C. Knie, M. Utrecht, F. Zhao, H. Kulla, S. Kovalenko, A. M. Brouwer, P. Saalfrank, S. Hecht, D. Bléger, *Chem. Eur. J.*, 2014, **20**, 16492; D. Bléger, J. Schwarz, A. M. Brouwer, S. Hecht, *J. Am. Chem. Soc.*, 2012, **134**, 20597.

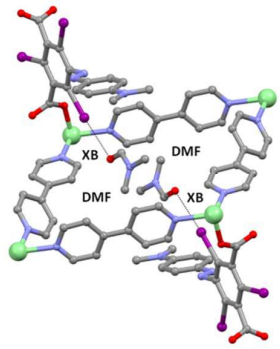

Coordination network decorated with halogen-bond donor sites for specific guest binding.